



Efficient self-metathesis of 1-butene on molybdenum oxide supported on silica modified one-dimensional γ -Al₂O₃

Yuming Cui^{a,1}, Na Liu^{a,b,1}, Yifen Xia^a, Jiangang Lv^a, Sujuan Zheng^a, Nianhua Xue^{a,*}, Luming Peng^a, Xuefeng Guo^a, Weiping Ding^{a,*}

^a Key Lab of Mesoscopic Chemistry, The School of Chemistry and Chemical Engineering, Nanjing University, Nanjing 210093, China

^b Department of Chemistry and Chemical Engineering, Xi'an University of Science and Technology, Xi'an 710054, China



ARTICLE INFO

Article history:

Received 4 April 2014

Received in revised form 18 June 2014

Accepted 23 June 2014

Available online 5 July 2014

Keywords:

Self-metathesis

1-Butene

Molybdenum oxides

One-dimensional γ -Al₂O₃

Silica modification

ABSTRACT

1-Butene, abundant but inexpensive in industry, can be used to produce more valuable propene and ethene through the well-known metathesis reaction. In terms of catalyst system of molybdena, controlling the interaction between the molybdena and the support is quite crucial. A special support, i.e., well-shaped one-dimensional γ -Al₂O₃ with uniform diameters of ~10 nm and lengths of ~100 nm, has been synthesized via oleylamine-assisted hydrothermal method. The molybdenum oxides are well controlled in sizes of moderate aggregation suitable for 1-butene metathesis with a fairly high rate of propene production (38.9×10^{-9} mol m⁻² s⁻¹, 30 mol% yield in a single pass) under mild conditions. The status of MoO_x species in the catalyst has been investigated by solid state ²⁹Si MAS NMR, Raman, UV-vis, H₂-TPR and NH₃-TPD techniques. The catalyst, highly stable after twelve times of regeneration, is important for practical utilization for the metathesis reactions.

© 2014 Elsevier B.V. All rights reserved.

1. Introduction

Propene is an important building block for important polymers, intermediates and chemicals. Alternative technologies for propene production have been attracted attention due to the fast increasing demand for propene, such as propane dehydrogenation, olefin metathesis, methanol to propene and cracking of low-value olefins. The first metathesis reactions were found by industrial chemists at Du Pont, Standard Oil and Phillips Petroleum (H.S. Eleuterio, E.F. Peters, B.L. Evering, R.L. Banks and G.C. Bailey) 60 years ago which offers new industrial routes to important petrochemicals, polymeric materials and pharmaceutical intermediates. It is now extensively explored in various reactions, such as ring-opening metathesis polymerization, ring-closing metathesis, acyclic diene metathesis polymerization and cross-metathesis [1–5]. Propene cannot be produced from only 1-butene over homogeneous (Grubbs first generation-type) ruthenium catalysts. To produce propene from 1-butene, 2-butene must be produced firstly

through isomerization reaction of 1-butene and then the metathesis reaction follows [1]. For the heterogeneous metathesis reaction, catalysts are commonly composed of Re, W or Mo elements which are active centers supported on high-surface-area alumina or silica [4,6–8]. The metal-carbene species are usually acknowledged as the initiating and propagating intermediates in olefin metathesis reaction, as described by the Herisson–Chauvin mechanism [9]. The key step of olefin metathesis is the formation of metal carbenes through the interaction between the alkene molecules and the transition metal centers. Hence, it is crucial to control the interaction between the active centers and the support for exploring the effective catalyst.

A large number of studies have focused on the interactions among the supports and the supported molybdena species [10–12]. Commonly, the molybdena/silica-alumina shows higher activity than molybdena loaded on alumina or silica alone [8,10–17]. Furthermore, the active sites are not highly dispersed Mo species but clusters composed of several molybdate species [18]. To pursue the efficiency of catalyst, a series of preparation methods have been developed, intending to control the interaction between metal centers and the supports. Recently, Debecker et al. have prepared molybdena catalysts using different methods in the liquid phase, such as one-pot aerosol route [19], the non-hydrolytic

* Corresponding authors. Tel.: +86 25 83595077; fax: +86 25 83317761.

E-mail addresses: nianhua@nju.edu.cn (N. Xue), dingwp@nju.edu.cn (W. Ding).

¹ These authors contributed equally to this work.

sol-gel catalysts of Si-Al-Mo mixed oxides [20], flame spray pyrolysis (FSP) synthesis and thermal spreading [21,22]. These investigations have demonstrated interesting and important results.

In the present work, a high performance catalyst with molybdena as active species and a kind of well-shaped one-dimensional $\gamma\text{-Al}_2\text{O}_3$ as the support is prepared for 1-butene self-metathesis. The catalyst shows ~40 mol% yield of propene and ethene at 393 K under 0.1 MPa with a high weight hourly space velocity (WHSV, 2.4 h^{-1}). The one-dimensional $\gamma\text{-Al}_2\text{O}_3$, uniform in size and morphology (10–20 nm of diameters and ~100 nm of lengths), supports most of the active molybdena species in suitable aggregation sizes. It offers quite active sites and is also stable during multi-regeneration for 1-butene metathesis.

2. Experimental

2.1. Catalyst preparation

2.1.1. One-dimensional $\gamma\text{-Al}_2\text{O}_3$ support

All chemical reagents were of analytical grade and used without further purification. One-dimensional $\gamma\text{-Al}_2\text{O}_3$ was prepared by hydrothermal synthesis method. Typically, oleylamine (80–90%, Aladdin Industrial Corporation) and $\text{NH}_3\text{-H}_2\text{O}$ (25%) was dissolved in distilled water at 353 K. The alumina sol (Zhejiang Yuda Chemical Industry Co., Ltd.) was then gradually added into the above solution under stirring for 2 h at 353 K. Then the mixture was transferred into the autoclave, which was sealed and maintained at 453 K for 72 h. After the reaction, the solids were collected, washed with distilled water and alcohol, then dried in the air at 373 K for 12 h and calcined at 823 K for 24 h. One-dimensional $\gamma\text{-Al}_2\text{O}_3$ was designated as Al(n).

2.1.2. Silica modification

Commercial $\gamma\text{-Al}_2\text{O}_3$ powder was obtained from Fu Shun Research Institute of Petroleum and Petrochemicals, China, which was designated as Al(c). The silica modified $\gamma\text{-Al}_2\text{O}_3$ was prepared according to the procedure reported elsewhere [23]. Typically, the samples of silica modified Al(c) and Al(n) were prepared by immersing 1 g of commercial $\gamma\text{-Al}_2\text{O}_3$ or one-dimensional $\gamma\text{-Al}_2\text{O}_3$ into an ethanol solution (20 mL) containing a certain amount of 3-aminopropyl-triethoxysilane (Aldrich, 99.9%) under stirring for 2 h at the room temperature. The obtained solid was dried and then calcined at 823 K for 12 h in air. They were designated as ySi/Al(c) and ySi/Al(n), respectively, where y is the SiO_2 loading in weight percent (wt.%).

2.1.3. MoO_3 loaded on ySi/Al(c) and ySi/Al(n)

The catalysts of supported molybdena were prepared by impregnating the supports, i.e. Al(c), Al(n), ySi/Al(c) and ySi/Al(n), with an appropriate amount of ammonium molybdate (AR) solution under stirring for 6 h, then dried at 373 K, and finally calcined at 823 K for 8 h in air. The prepared catalysts were denoted as xMo/ySi/Al(c) and xMo/ySi/Al(n), respectively, where x is the MoO_3 loading in weight percent (wt.%). The catalysts were pressed and crushed to particles of 20–40 mesh for 1-butene metathesis reaction and performed corresponding characterization.

2.2. Catalytic test

The 1-butene metathesis reaction was carried out in a continuous-flow, fixed-bed system. 0.2 g of catalyst was placed onto a quartz wool plug located in a quartz U-tube. After the catalyst was pretreated at 873 K for 2 h under Ar (99.9%, 60 mL min^{-1}), then cooled down to the desired reaction temperatures in the Ar flow

and the 1-butene (99.5%) was introduced to the reaction system. The reaction conditions were as following: 393 K, 0.1 MPa, 2.4 h^{-1} of WHSV ($1\text{-C}_4\text{H}_8$). The reaction products were analyzed online by gas chromatography equipped with a 50-m fused silica chrompack PLOT $\text{Al}_2\text{O}_3/\text{Na}_2\text{SO}_4$ capillary column and a flame ionization detector. Regeneration of the used catalysts was performed at 823 K for 6 h in the atmosphere of oxygen.

A series of reaction pathways have been observed in the self-metathesis of 1-butene on catalysts: isomerization, self-metathesis, cross-metathesis, secondary cross-metathesis and oligomerization [24]. We classify alkene products as C_n^- , where n represents the carbon numbers. The conversion $X(C_n^-)$ is determined by subtracting the mass percentage of 1-butene feed in the blank effluent gas, as Eq. (1).

$$(1) X(C_1^-) = \frac{W_{1\text{-butene}}^{\text{blank}} - W_{1\text{-butene}}^{\text{outlet}}}{W_{1\text{-butene}}^{\text{blank}}}$$

$W_{1\text{-butene}}^{\text{blank}}$: 1-butene feed from the blank reaction

$W_{1\text{-butene}}^{\text{outlet}}$: 1-butene feed from the outlet after reaction

The molar yield of the product is calculated according to following Eq. (2):

$$(2) Y(C_n^-) = \frac{X(C_n^-) \times ((W(C_n^-)/n))}{((W(C_2^-))/2) + (W(C_3^-))/3) + (W(C_4^-))/4) + (W(C_5^-))/5) + (W(C_6^-))/6) + (W(C_7^-))/7)}$$

where $W(C_n^-)$ is the mass percent of the product with the given carbon number, and $Y(C_n^-)$ is the molar yield. C_7^- is used to denote all the polymerized alkenes with carbon numbers over six. The specific activity is defined as the number of moles of propene produced during the reaction per m^2 of the catalyst and per second.

2.3. Characterization

XRD patterns of the samples were recorded in the 2θ region of $10\text{--}80^\circ$ using a diffractometer (Shimadzu XRD-6000) with $\text{Cu K}\alpha$ radiation ($\lambda = 1.5418\text{ \AA}$). The scan speed was set at $10^\circ \text{ min}^{-1}$ with a step size of 0.02° .

The specific surface areas and pore volumes of catalysts were obtained by means of the nitrogen adsorption measurement at 77 K on a Micrometrics ASAP 2020 instrument. Samples were outgassed at 573 K ($<10^{-3}$ Torr) for 4 h prior to analysis. Adsorption data were analyzed by the Barrett-Joyner-Halenda (BJH) method. Pore-size distribution curves were calculated using the Dolimore-Heal (D-H) method.

TEM measurements were conducted with JEOL JEM-100S, using an accelerating voltage of 80 kV. Samples for TEM measurements were suspended in ethanol and ultrasonically dispersed. Drops of the suspensions were applied to a carbon-coated copper grid. FTIR spectra of catalysts were obtained on a FT-IR spectrometer (Bruker Vector 22) with a resolution of 4 cm^{-1} at room temperature. Raman spectra were recorded with a Renishaw inVia system equipped with a confocal microscope. A 514.5 nm exciting line was focused using a $50\times$ objective lens. The laser power at the sample was 20 mW. Diffuse reflectance UV-vis spectra were recorded with a UV-2401PC spectrometer under air-exposed conditions in the range 200–800 nm. The scan speed was 120 nm min^{-1} and the BaSO_4 powder was used as the reference.

$\text{NH}_3\text{-TPD}$ profiles were obtained by using a micromeritics AutoChem TP-5080 apparatus with a thermal conductivity detector (Tianjin Golden Eagle Technology Limited Corporation). Prior to measurement, 0.1 g of the sample was pretreated in a helium flow at 873 K for 2 h and then cooled down to 373 K. Subsequently a flow of ammonia/helium mixed gas (5 vol.% ammonia) was passed and maintained for 30 min. Then the excess ammonia was removed by a helium flow at 373 K for 1 h. The ammonia desorption was performed in the temperature range of 373–873 K at a rate of 10 K min^{-1} . The desorbed NH_3 was detected using a thermal conductivity detector (TCD).

Temperature-programmed reduction of H_2 ($\text{H}_2\text{-TPR}$) measurements were carried out in a conventional setup (Tianjin Xianquan

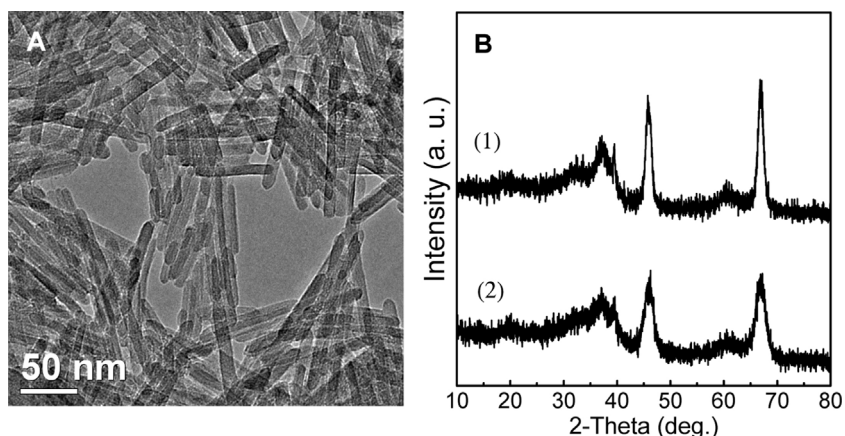


Fig. 1. (A) The TEM image of the one-dimensional γ -Al₂O₃; (B) XRD patterns of (1) one-dimensional γ -Al₂O₃ and (2) commercial γ -Al₂O₃.

Industry and Trade Development Co., Ltd). Prior to measurements, the sample was pretreated at 823 K for 2 h in an He flow and then cooled to the room temperature. H₂-TPR profiles were obtained with a thermal detector in the range of ambient to 1073 K at a programmed temperature rate of 10 K min⁻¹ under a 5 vol.% H₂/N₂ flow (30 mL min⁻¹).

TG analysis of used catalysts was carried out on a STA 449C-Thermal star instrument to monitor the amount of coke deposition in the catalytic process. The catalyst loading was about 10 mg and the gas flow was 20 mL min⁻¹. The catalyst was heated from room temperature to 1073 K in air stream at a heating rate of 10 K min⁻¹.

Temperature programmed oxidation (O₂-TPO) was performed with a mass spectrometer (Inficon Transpector 2) to investigate the coke formation. The 0.1 g of catalyst was heated from room temperature to 973 K in a 10% O₂/Ar flow (100 mL min⁻¹) at a heating rate of 10 K min⁻¹, during which m/e intensities for CO₂(44), CO(28), O₂(32), and H₂O(18) were recorded. Argon was used as an internal standard in order to calculate the amount of CO, CO₂ and H₂O.

²⁹Si MAS NMR experiments were performed on a Bruker Avance III spectrometer in a magnetic field strength of 9.4 T at the resonance frequency of 79.5 MHz. The spectra were recorded using a 7 mm MAS probe with a $\pi/2$ pulse length of 4.5 μ s, the recycle delay is 15 s at a spinning rate of 6 kHz. The chemical shift was referenced to DSS (4,4-Dimethyl-4-silapentane-1-sulfonic acid sodium salt) at 1.534 ppm.

Table 1
BET surface areas and catalytic performances of prepared catalysts.

Catalysts	S _{BET} (m ² g ⁻¹)	1-C ₄ ^a Con. (mol%)	Yield of products (mol%)					TOF ^a (mmol mol ⁻¹ s ⁻¹)	Area activity ^b ($\times 10^{-6}$ mmol m ⁻² s ⁻¹)	Specific activity ^c (mmol g ⁻¹ h ⁻¹)
			C ₂ ^a	C ₃ ^a	C ₅ ^a	C ₆ ^a	2-C ₄ ^a			
0Mo/Al(c)	180	2.8	0	0	0	0	2.8	0	0	0
0Mo/Al(n)	148	2.6	0	0	0	0	2.6	0	0	0
0Mo/4Si/Al(c)	167	5.6	0	0	0	0	5.6	0	0	0
0Mo/4Si/Al(n)	124	15.6	0	0	0	0	15.6	0	0	0
10Mo/Al(c)	168	23.3	1.1	3.0	2.6	1.3	10.5	0.73	2.10	1.28
10Mo/Al(n)	138	31.9	1.2	3.1	2.9	1.6	23.1	0.76	2.70	1.33
10Mo/4Si/Al(c)	160	31.5	5.0	6.5	5.3	6.6	8.1	1.59	4.80	2.78
10Mo/2Si/Al(n)	130	55.0	4.0	19.6	16.5	5.1	9.8	4.80	17.9	8.38
1Mo/4Si/Al(n)	120	30.0	0.8	4.3	3.9	1.2	17.8	7.76	4.30	1.84
6Mo/4Si/Al(n)	109	69.3	2.3	23.2	19.7	3.8	20.3	7.37	25.3	9.92
10Mo/4Si/Al(n)	92	82.0	7.0	30.2	27.2	9.8	7.8	7.40	38.9	12.9
20Mo/4Si/Al(n)	66	32.3	0	0	0	0	32.3	0	0	0
10Mo/10Si/Al(n)	80	27.8	0	0	0	0	27.8	0	0	0

Reaction conditions: catalyst = 0.2 g, T = 393 K, P = 0.1 MPa, WHSV (1-C₄H₈) = 2.4 h⁻¹, time on stream = 1 h.

^a The apparent turnover frequency (TOF) is defined as the number of millimole of propene produced per mole of Mo (considering the total Mo content) and per second (mmol mol⁻¹ s⁻¹).

^b The area activity is calculated as the number of mmoles of propene produced per m² of catalyst and per second (units: $\times 10^{-6}$ mmol m⁻² s⁻¹).

^c The specific activity is defined as the number of mmoles of 1-butene converted and products formed per gram of catalyst and per hour (mmol g⁻¹ h⁻¹).

3. Results and discussion

3.1. Composition and structure of the catalysts

The TEM result listed in Fig. 1A reveals that the Al(n) sample presents a highly uniform size with diameters of \sim 10 nm and lengths of \sim 100 nm. The XRD patterns of the supports shown in Fig. 1B indicate that both commercial γ -Al₂O₃ and one-dimensional γ -Al₂O₃ exhibit two broad diffraction peaks at 45.9° and 67.1° in the region between 10° and 80° which correspond to characteristic peaks of γ -Al₂O₃ (JCPDS: 10-0425). The specific surface area of one-dimensional γ -Al₂O₃ is slightly smaller than that of the commercial γ -Al₂O₃. Introducing silica to the both alumina samples results in the decrease of the surface areas. Further decrease of surface areas of samples is presented in all molybdena doped silica-alumina samples (Table 1).

After loading molybdena, XRD patterns of the prepared catalysts are depicted in Fig. 2. The structure and the crystalline properties of γ -Al₂O₃ are remained unchanged upon silica deposition. No any diffraction lines corresponding to Mo compounds are detected on catalysts with low MoO₃ loadings (\leq 10 wt.%). This suggests that the Mo species are relatively high dispersed over the supports. When 20 wt.% of MoO₃ is loaded, the characteristic peaks of crystalline MoO₃ diffraction appear at 23.4°, 25.8°, 27.4°, corresponding to the orthorhombic crystalline MoO₃ (α -MoO₃) [21].

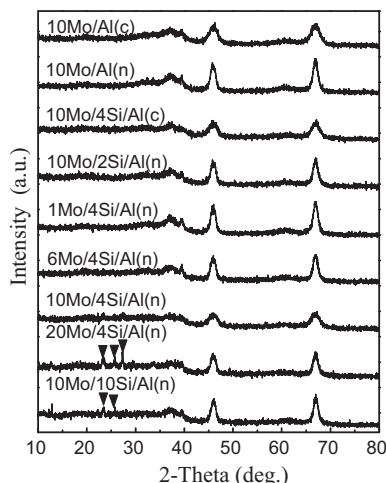


Fig. 2. XRD patterns of molybdenum oxides supported on silica modified alumina. Al(c): commercial γ -Al₂O₃ powder; Al(n): one-dimensional γ -Al₂O₃. (▼) α -MoO₃.

3.2. ^{29}Si MAS NMR

To characterize the dispersion of silica on alumina surface, the ^{29}Si MAS NMR measurements are performed and the spectra of 4Si/Al(n) and 4Si/Al(c) are shown in Fig. 3. The resonance at around $-102\text{--}-116$ ppm can be assigned to the crystallographically equivalent site of the Si(OSi)₄ (Q4) group [6]. The resonances in the range of -78 and -83 ppm can be tentatively assigned to Si(OSi)₂(OH)₂ and Si(OAl)₃OH, respectively [25]. The ^{29}Si MAS NMR spectrum of the 4Si/Al(n) shows the stronger intensity of resonances at -78 and -83 ppm and the weaker intensity of the resonances at $-102\text{--}-116$ ppm compared with 4Si/Al(c). From above, the fraction of Q4 is much higher on commercial alumina than one-dimensional alumina, hence the dispersion of silica over γ -Al₂O₃(n) is much better than over γ -Al₂O₃(c). In terms of silica modified alumina, deposition of multiple layers of silica would be expected to lead to a nonacidic surface, similar to pure amorphous silica [26]. Niwa et al. reported that in the boundary layer between alumina and silica, the species assumed or the substituted aluminum cation like in zeolite framework could be formed to play the role of the Brønsted acid site [27]. In the present work, the silica with good dispersion which is nearly atomic dispersion in one-dimensional

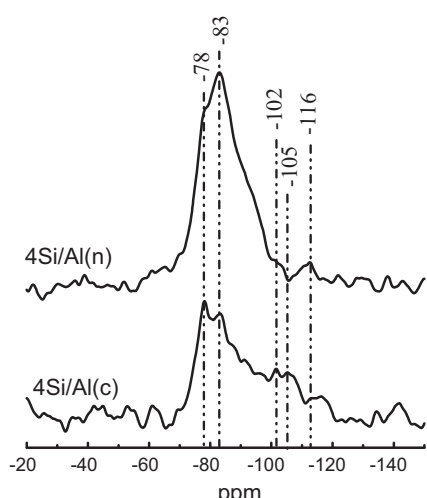


Fig. 3. ^{29}Si MAS NMR spectra of 4Si/Al(c) and 4Si/Al(n). Al(c): commercial γ -Al₂O₃ powder; Al(n): one-dimensional γ -Al₂O₃.

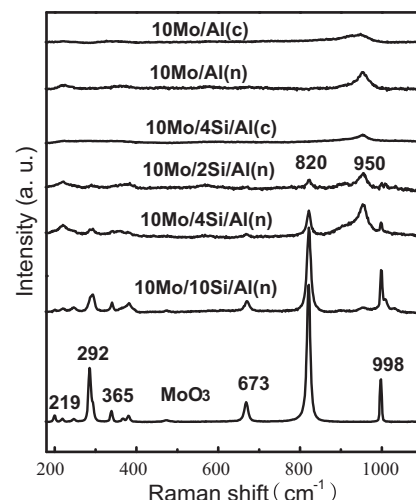


Fig. 4. Raman spectra of the catalysts. Al(c): commercial γ -Al₂O₃ powder; Al(n): one-dimensional γ -Al₂O₃.

γ -Al₂O₃ surface is expected to possess more abundant boundary layer offering more Brønsted acid sites.

3.3. Raman spectroscopy

From the Raman spectra shown in Fig. 4, the bulky MoO₃ itself gives several sharp signals. The 292 cm^{-1} band is a doublet comprised of wagging modes of the terminal oxygen connected to Mo atoms. The band centered at 673 cm^{-1} is an asymmetric stretching of the Mo-O-Mo along *c* axis. The peak centered at 820 cm^{-1} is due to the antisymmetric stretching mode of O-Mo-O. The band at 998 cm^{-1} is from asymmetric stretch of the terminal oxygen atoms (Mo=O) [28,29]. With the both alumina as the supports, even 10 wt.% molybdena presents very weak Raman signals related to crystalline MoO₃. However, only one small broad band at $\sim 950\text{ cm}^{-1}$ was observed (Fig. 4), which is assigned to two-dimensional MoO_x oligomers dispersed on the both alumina supports, implying the strong interaction of molybdena with the alumina supports and high dispersion of molybdena [4]. For 10Mo/4Si/Al(c), Raman signals related to crystalline molybdena are not observed even with the silica modification except signals at 950 cm^{-1} to MoO_x oligomers. However, the weak but clear signals related to aggregated molybdena emerge in 10Mo/4Si/Al(n) sample. This reveals the relative weaker interaction between Mo species and silica modified one-dimensional alumina than commercial one. Increasing silica loading, i.e. 10Mo/10Si/Al(n), sharp signals centered around $\sim 999\text{ cm}^{-1}$ (Mo=O stretching), $\sim 950\text{ cm}^{-1}$ (terminal M=O stretch mode in MoO_x oligomers), $\sim 822\text{ cm}^{-1}$ (antisymmetric stretching mode of Mo-O-Mo), $\sim 673\text{ cm}^{-1}$ and a broad band at $210\text{--}350\text{ cm}^{-1}$ (Mo=O bend) are detected, implying bulky MoO₃ crystals presented in the surface. This is due to the weakened interaction between the support and the molybdena species by the thick layer of silica on the alumina surface.

3.4. UV-vis spectrum

The optical bandgap energy, E_g , determined from the position of the low energy rise in UV-vis spectrum of prepared material could characterize the average particle size of domains of transition metal oxides [28]. The absorption edge is defined as the *x*-intercept of the straight line describing the near-edge region for spectra plotted as $[F(R_\infty)hv]^2$ as a function of hv , where $F(R_\infty)$ is the Kubelka–Munk function and hv is the energy of the incident photon. The absorption edge energy decreases with increasing domain

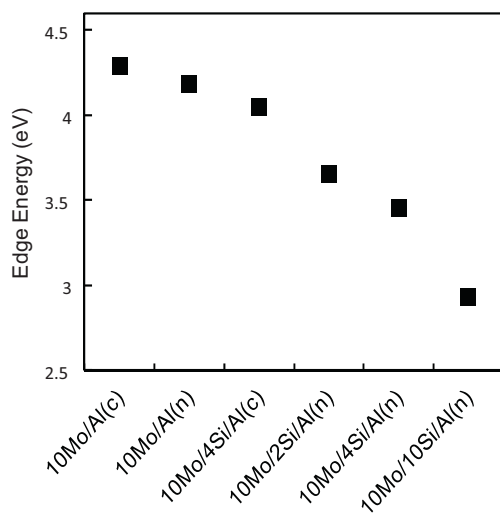


Fig. 5. The UV-vis absorption edge energies of the prepared catalysts with the same Mo surface density on different supports. Al(c): commercial γ - Al_2O_3 powder; Al(n): one-dimensional γ - Al_2O_3 .

size. The UV-vis absorption edge energies of the prepared catalysts with the same Mo surface density on different supports are shown in Fig. 5. Comparing 10Mo/Al(c) with 10Mo/Al(n), it reveals that the sizes of MoO_3 species in 10Mo/Al(c) are smaller than those in 10Mo/Al(n). A decrease in absorption edge energy emerges when MoO_x species are supported on silica modified alumina. The size of MoO_x species in $y\text{Si}/\text{Al}(n)$ surface increases with the increase of the silica content in $\gamma\text{-Al}_2\text{O}_3$. The higher absorption edge energy of 10Mo/4Si/Al(c) is presented compared with that of 10Mo/4Si/Al(n), which reflects the smaller MoO_x clusters in the former sample.

3.5. Temperature-programmed reduction of H_2 (H_2 -TPR)

It is well accepted that olefin metathesis reaction follows metal carbene mechanism over heterogeneous catalysts. Therefore, the redox property of the Mo species in catalyst surface plays an important role in the metathesis reaction. H_2 -TPR measurements could offer the information on the supported Mo species. The TPR profiles of the prepared catalysts are shown in Fig. 6. Two reduction peaks in the range of 700–780 K and 1123–1183 K are observed for both 10Mo/Al(c) and 10Mo/Al(n) samples. The peak at low temperature (700–780 K) is generally associated with the reduction of well dispersed octahedral Mo^{6+} to Mo^{4+} species [14,16]. The one at high temperatures is attributed to a further progress in the reduction of partially reduced MoO_x species formed in the first reduction process, together with the partial reduction of tetrahedrally coordinated Mo species strongly interacting with Al_2O_3 [30].

In addition to the two peaks abovementioned on alumina supported Mo oxides, two shoulder peaks in the range of 850–950 K and 1000–1100 K appear over the molybdenum oxides supported

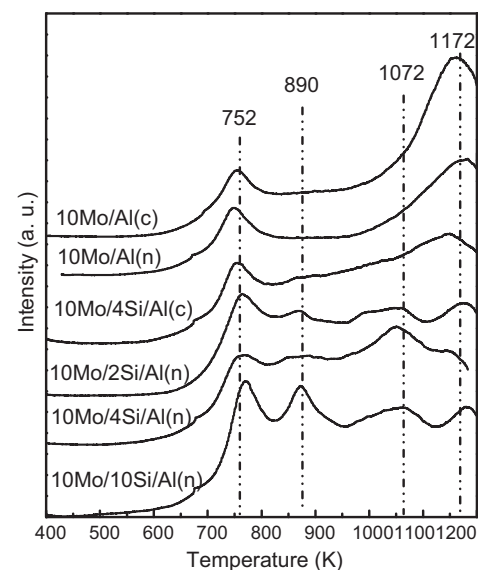
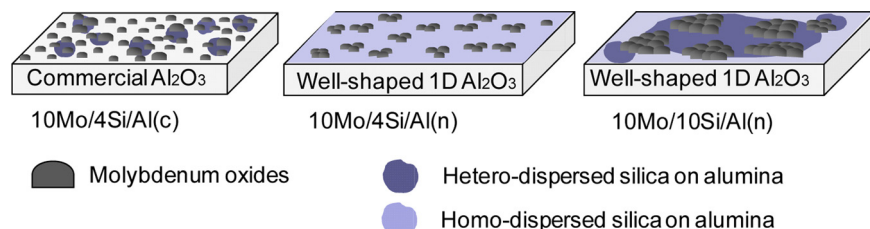


Fig. 6. H_2 -TPR profiles of the Mo catalysts with different supports. Al(c): commercial γ - Al_2O_3 powder; Al(n): one-dimensional γ - Al_2O_3 .

on silica modified alumina catalysts (Fig. 6). The first shoulder peak (850–950 K) is attributed to the reduction of microcrystalline MoO_3 to MoO_2 [31]. The other peak between 1000 K and 1100 K should be attributed to the reduction of the molybdenum oxide in lower levels of aggregation. From above results, there are more molybdena species easily reduced which are in polymeric or microcrystalline state on the support surface on the silica modified one-dimensional $\gamma\text{-Al}_2\text{O}_3$ than commercial one. Further increasing silica content on the Al(n) surface, the hydrogen consumption increases due to the increased amount of the easily reduced molybdena species, which is the molybdena species aggregated to some extent. The amount of molybdena species strongly interacted with the support and difficult to be reduced decreases with the increase in silica content.

The dispersion of the silica in alumina (Al(c) and Al(n)) directly influences the status of supported molybdena. When the loading of silica is lower than one monolayer (~4 wt.%) over the one-dimensional $\gamma\text{-Al}_2\text{O}_3$, the MoO_x species are highly dispersed on it owing to strong interaction with the hydroxyl of alumina surface [32]. Maybe due to its unique surface structure, the well-shaped one-dimensional $\gamma\text{-Al}_2\text{O}_3$ sample can support the silica modified in highly dispersed state. The sample Al(c) cannot support the highly homogeneous dispersion of silica for the heterogeneity of its surface. The special surface property of 4Si/Al(n) with homogeneously dispersed silica sets the MoO_x species in certain sizes of polymerization which might be with special performance toward olefin metathesis. The catalyst structures are schematically shown in Scheme 1, which is also deduced with the spectroscopic results of Raman, UV-vis and H_2 -TPR measurements.



Scheme 1. Schematic show of MoO_x species dispersed on silica modified commercial γ - Al_2O_3 powder (presented by Al(c)) and one-dimensional γ - Al_2O_3 (presented by Al(n)).

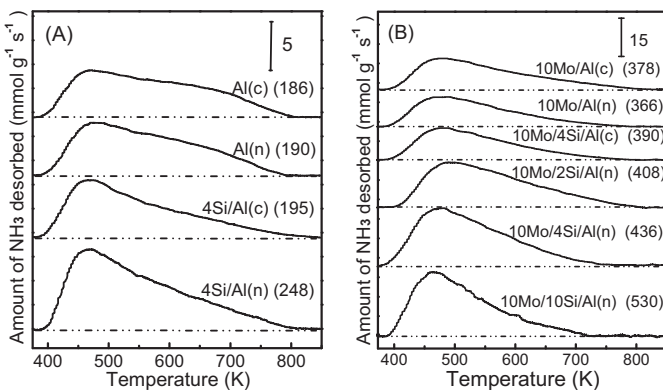


Fig. 7. NH₃-TPD of the catalysts: (A) supports; (B) molybdena supported on different supports. The number in the parenthesis presents the amount of desorbed NH₃ ($\mu\text{mol g}^{-1}$). Al(c): commercial $\gamma\text{-Al}_2\text{O}_3$ powder; Al(n): one-dimensional $\gamma\text{-Al}_2\text{O}_3$.

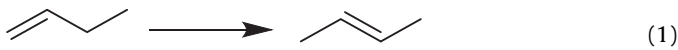
3.6. Ammonia temperature-programmed desorption (NH₃-TPD)

It has been reported that the stability of catalysts with time on stream is governed at least in part by the acidity of the catalysts [13]. Fig. 7A shows the NH₃-TPD profiles of the supports used in the present work. A main desorption peak centered at about 450 K with a long tail is observed for all the supports. The Al(c) and Al(n) possess similar quantity of adsorbed ammonia. However, more acid sites are detected in Al(n) than that in Al(c) when doping 4 wt.% silica to the alumina surface. This reveals that silica in one-dimensional $\gamma\text{-Al}_2\text{O}_3$ disperses better than in commercial alumina to more interface of silica–alumina which probably offers Brønsted acid sites [33]. When adding Mo species to these varied supports, the amount of adsorbed ammonia dramatically increases (Fig. 7B). For silica modified Al(n), introducing 10 wt.% MoO₃ species results in different increase of detected acid sites with different silica content. More silica in Mo/Al(n) leads to more acid sites detected. The detected acid sites should include Lewis (bare Mo atom, terminal oxygen vacancy), Brønsted acid sites (Mo-OH) in MoO₃ clusters formed in alumina surface and Brønsted acid sites from silica–alumina interface [33]. According to the total amount of acid sites detected by NH₃-TPD, 10Mo/4Si/Al(n) and 10Mo/10Si/Al(n) presented relatively higher density of acid sites. Based on the relationship among the acidity, activity and stability of the catalysts [13,34], the better activity and stability is expected on the molybdena catalysts supported on silica modified one-dimensional $\gamma\text{-Al}_2\text{O}_3$ for the metathesis reaction.

3.7. 1-Butene metathesis reaction

A series of reaction pathways have been demonstrated in the self-metathesis of 1-butene on the catalysts [24]. The reaction pathways of 1-butene on molybdena supported on alumina are listed as follows.

Isomerization:



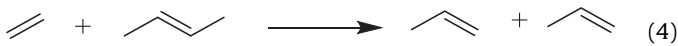
Self-metathesis:



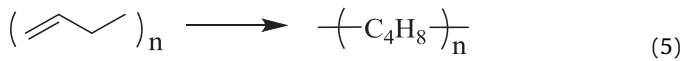
Cross-metathesis:



Secondary cross-metathesis:



Oligomerization:



The main products are ethene, propene, pentene, hexene, 2-butene and minor C₇₊ hydrocarbons. Propene and pentene are the products of cross-metathesis reaction of 1-butene and 2-butene and secondary cross-metathesis of ethene and 2-butene. Among products, 2-C₄⁼ represents isomerization of 1-butene. C₅⁼ represents substances bearing five carbon atoms, which are mainly produced from secondary metathesis. C₆⁼ is used to denote the alkenes with six carbon atoms, which are produced from self-metathesis. For clarity, the minor C₇₊ alkenes (<2.5 mol%) are omitted in the presented table of products (Table 1).

From the data in Table 1, both commercial and one-dimensional $\gamma\text{-Al}_2\text{O}_3$ do not present metathesis activity but low isomerization activity because of no Brønsted acid sites in alumina. After loading silica to the two supports, there is still no metathesis activity with the increased isomerization activity. Both Mo/Al(c) and Mo/Al(n) present metathesis activity with the increased isomerization activity simultaneously. However, the metathesis products are in low yields due to the excessive dispersion of the MoO₃ species and the poor acidity of the catalysts [34]. This is also fairly consistent with the results of a low activity for Mo/ $\gamma\text{-Al}_2\text{O}_3$ documented [35].

Among the prepared catalyst, the 10Mo/4Si/Al(n) catalyst presents the highest activity with a 82.0 mol% conversion of 1-butene, which corresponds to the production of propene and ethene with a 40 mol% yield at the high space velocity of 2.4 h⁻¹ (WHSV) at 393 K. Excessive silica in alumina surface makes the larger crystalline of molybdenum oxides in the catalyst surface, such as in 10Mo/10Si/Al(n), which is less active in metathesis reaction. On the other hand, when the molybdena content reaches 20 wt.% on the 4Si/Al(n) surface, the bulky Mo species form and are inactive for the metathesis reactions [36]. Thomas et al. have also reported that the catalytic activity of MoO₃/Al₂O₃ is highly dependent on the molybdena loading. The catalytic activity firstly increases with the surface coverage of molybdena, then passes through a maximum one [37]. Comparing with other reports on 1-butene self-metathesis reactions (Table 2), molybdena supported on silica modified one-dimensional $\gamma\text{-Al}_2\text{O}_3$ catalysts shows the highest activity of 1-butene metathesis activity (high specific activity, $38.9 \times 10^{-9} \text{ mol m}^{-2} \text{ s}^{-1}$) at atmospheric pressure and low reaction temperature.

The bi-functional sites in moderate aggregated molybdena species supported on the silica modified one-dimensional $\gamma\text{-Al}_2\text{O}_3$ are responsible for the isomerization and metathesis simultaneously. Combing the results of Raman, UV-vis spectra with the metathesis activity of 1-butene, it is concluded that the metathesis reaction is complicated. The acidity and reducibility of the prepared supported molybdena catalysts are both contributed to the catalytic activity [37]. In current research, the MoO_x species are quite highly dispersed, which are difficult to reduce, on Al(c), Al(n), 4Si/Al(c) due to the strong interaction between the Mo species and supports. These catalysts are less active for the reaction. On the other hand, the high activity of the 10Mo/4Si/Al(n) is correspondingly related to the mildly aggregated MoO_x species and suitable reducibility and the relatively stronger acid of the 4Si/Al(n) plays a role for the isomerization of 1-butene to 2-butene. The integrative effects result in a good catalyst 10Mo/4Si/Al(n).

3.8. Deactivation and regeneration of the 10Mo/4Si/Al catalyst

The effect of space velocity on the reaction performance of 10Mo/4Si/Al(n) at 393 K is summarized in Fig. 8. Although the space velocities of 1-butene are different, the initial conversion and yields of metathesis products are similar. The regeneration cycle shortens

Table 2

The metathesis activity of heterogeneous Mo and W based catalysts for 1-butene transformation reported in references.

Catalyst	T (K)	P (MPa)	Space velocity	C_3^{\equiv} yield (mol%)	TOF ^a (mmol mol ⁻¹ s ⁻¹)	Area activity ^b ($\times 10^{-6}$ mmol m ⁻² s ⁻¹)	Specific acitivity ^c (mmol g ⁻¹ h ⁻¹)	Refs.
Mo/HM-Al ₂ O ₃	423	0.1	1.5 ^d	26.5	3.54	8.8	7.1	[24]
Mo/M-Al ₂ O ₃	423	0.1	2.0 ^d	27.4	6.51	9.7	9.8	[4]
W/SiO ₂ /Al ₂ O ₃	453	0.1	2.4 ^d	20.9	9.59	18.2	8.9	[23]
WO ₃ /SiO ₂	623	0.5	0.36 ^d	18.96	1.31	1.7	1.2	[17]
WO ₃ /SBA-15	523	0.5	0.72 ^d	27.1	1.96	1.4	3.5	[8]
WO ₃ /SiO ₂ -Al ₂ O ₃	723	0.085	450 ^e	31.7	9.5	13.3	11.8	[5]
10Mo/4Si/Al(n)	393	0.1	2.4 ^d	30.2	7.40	38.9	12.9	Our

^a The apparent turnover frequency (TOF) is defined as the number of moles of propene produced per mole of Mo (considering the total Mo content, even if only part of the Mo is actually active) and per second (mmol mol⁻¹ s⁻¹).

^b The area activity is calculated as the number of mmoles of propene produced per m² of catalyst and per second (units: $\times 10^{-6}$ mmol m⁻² s⁻¹).

^c The specific activity is defined as the number of mmoles of 1-butene converted and products formed per gram of catalyst and per hour (mmol g⁻¹ h⁻¹).

^d WHSV (h⁻¹).

^e GHSV (mLh⁻¹ mL⁻¹).

with the increasing reaction space velocity of 1-butene. The performance of the catalyst begins to decrease after 24 h reaction with 1-butene space velocity at 0.6 h⁻¹. The catalytic performance of the catalyst can be stable to 12 h when the space velocity of 1-butene increases to 2.4 h⁻¹. The deactivation might be related to the coke deposition in the reaction process. However, 10Mo/4Si/Al(n) catalyst shows faster deactivation and lower yield of propene compared with 10Mo/4Si/Al(n) under the same reaction conditions.

The 10Mo/4Si/Al(n) catalyst shows good metathesis activity with a 1-butene conversion up to 82 mol% and a yield of propene and ethene up to ~40 mol% in 15 h reaction, as shown in Fig. 8C. The catalyst deactivates completely after 25 h reaction. Spamer et al.

has reported that the amount of coke formation is a critical factor in controlling the lifetime of WO₃/SiO₂ in the metathesis reaction of 1-heptene [38]. At the same time, the oxidation state of transition metal centers could be changed during the reaction, which may also influence the catalyst activity [15]. Thermal gravimetric (TG) analysis is used to determine the amount of coke on the catalyst. The corresponding TG profile of the used 10Mo/4Si/Al(n) is shown in Fig. 9A. Two weight loss steps could be observed on the catalyst after 25 h reaction. The first weight loss occurs at a temperature range between 300 K and 450 K, which is attributed to the desorption of water in catalyst. The second one is observed at a temperature range between 500 K and 850 K due to burning off coke

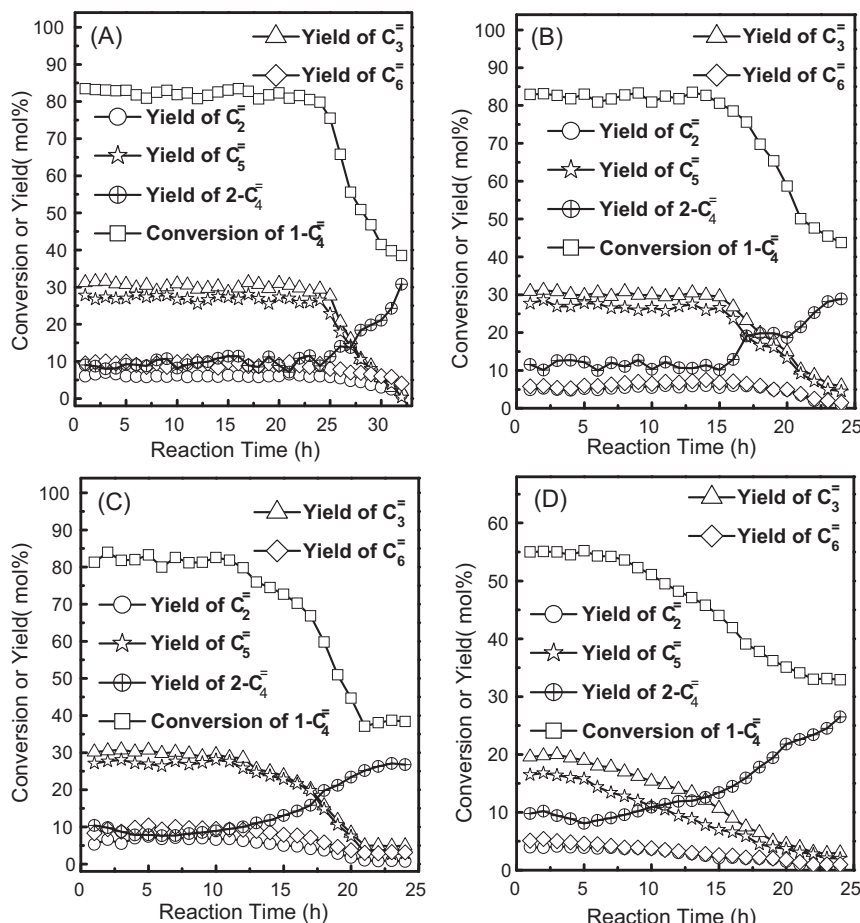


Fig. 8. Catalytic performance of 10Mo/4Si/Al(n) catalysts with the time on 1-butene stream at different space velocities and the performance of 10Mo/4Si/Al(c) (A) 0.6 h⁻¹, 10Mo/4Si/Al(n); (B) 1.2 h⁻¹, 10Mo/4Si/Al(n); (C) 2.4 h⁻¹, 10Mo/4Si/Al(n); (D) 2.4 h⁻¹, 10Mo/4Si/Al(c). (Catalyst = 0.2 g, T = 393 K, P = 0.1 MPa).

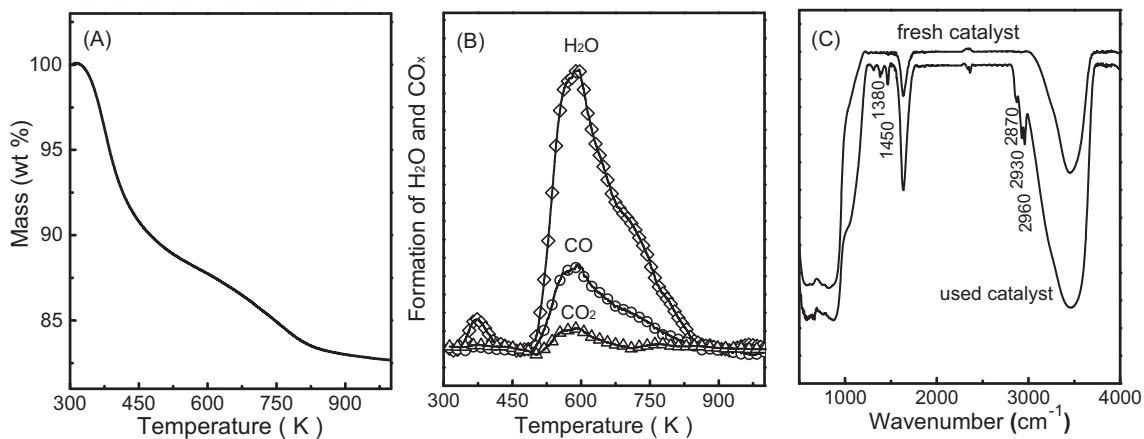


Fig. 9. (A) The TG profiles of 10Mo/4Si/Al(n) after 25 h reaction. (B) TPO profiles of 10Mo/4Si/Al(n) after 25 h reaction (100 mL min⁻¹ 10% O₂/Ar mixture; heating rate 10 K min⁻¹). (C) FTIR spectra of the fresh and used 10Mo/4Si/Al(n).

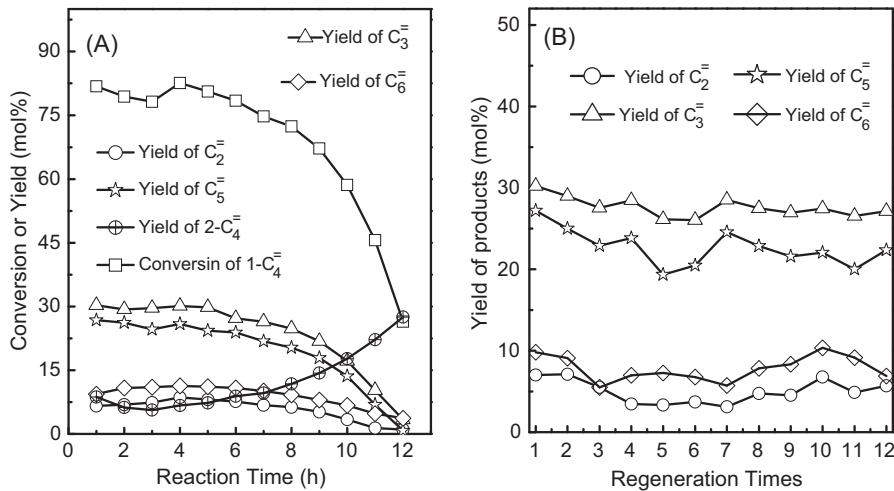


Fig. 10. (A) Catalytic performance of regenerated 10Mo/4Si/Al(n) in 1-butene metathesis reaction as a function of time on stream (Catalyst = 0.2 g, T = 393 K, P = 0.1 MPa, WHSV of 1-butene = 2.4 h⁻¹). (B) Catalytic performance of the regenerated catalyst (Catalyst = 0.2 g, T = 393 K, P = 0.1 MPa, WHSV of 1-butene = 2.4 h⁻¹, reaction time = 1 h).

formed in catalyst. Temperature programmed oxidation (TPO) profile of the used 10Mo/4Si/Al(n) is shown in Fig. 9B. There are two water signals centered at 350 K from the desorption of adsorbed water and at 590 K from the combustion of coke deposits in catalyst. The gases of CO and CO₂ begin to produce above 500 K and diminish at 850 K which is corresponding to the second weight loss of TG results. From these results, the amount of coke on 10Mo/4Si/Al(n) is about 7 wt.% after 24 h reaction.

FTIR is an efficient tool to study the nature of the coke on catalysts [39]. The FTIR spectra of fresh and used catalysts are shown in Fig. 9C. There are five new peaks appeared after 24 h metathesis reaction for 10Mo/4Si/Al(n) compared with the fresh one. The peaks at 2870 cm⁻¹, 2930 cm⁻¹, 2960 cm⁻¹ are assigned to stretch vibrations of –CH₃, –CH₂, –CH groups, as previously reported by Eberly et al. [40]. The band at 1450 cm⁻¹ corresponds to asymmetric deformations of –CH₃ groups and symmetric deformations of =CH₂ groups [41]. The band at 1380 cm⁻¹ is assigned to symmetric deformations of –CH₃ [42]. There is no band at 3050 cm⁻¹, corresponding to stretch vibration of the C–H bond of aromatics. The results indicate that the coke on used catalyst may be long chain alkenes formed by side reaction of olefin-oligomerization [15]. After regeneration at 823 K in air to remove the carbonaceous deposits, the used 10Mo/4Si/Al(n) catalyst recovers the metathesis performance again with unchanged conversion of 1-butene and yields of propene and ethene. The reusability of the catalyst for the

metathesis of 1-butene has also been carried out for several runs (Fig. 10B). It is worth to note that the yield of the propene and ethene remains basically even after regeneration of as many as 12 times.

4. Conclusions

The catalyst, molybdena supported on well-shaped one-dimensional γ-Al₂O₃ with homogeneously dispersed silica modification, exhibits a higher rate per mol of Mo atoms for 1-butene metathesis than on commercial γ-Al₂O₃. The uniform morphology of the one-dimensional γ-Al₂O₃ support is beneficial to disperse the silica homogeneously and sets the moderate interaction between MoO_x species and the support surface, which causes molybdenum oxides well dispersed in suitable aggregation states active and stable for 1-butene metathesis. At the same time, the silica modified one-dimensional γ-Al₂O₃ also offers suitable acidity for the isomerization of 1-butene to 2-butene. With these merits, the catalyst 10Mo/4Si/Al(n) shows highly catalytic performance for 1-butene metathesis to propene and ethene at mild conditions. The deactivated catalyst due to the deposition of long chain alkenes formed by the side reaction of olefin-oligomerization can be regenerated through calcination in air to remove the carbonaceous deposits and the initial activity of 1-butene conversion could be restored. The

thoughts of the catalyst design reported in the current work should be useful to develop an excellent metathesis catalyst applicable in the industrial process.

Acknowledgments

The project is supported by the Fundamental Research Funds for the Central Universities (Grant 1124020512, 1107020524), NSF of China (21103087, 21273107).

References

- [1] J.C. Mol, *J. Mol. Catal. A: Chem.* 213 (2004) 39–45.
- [2] J. Handzlik, K. Kurleto, *Curr. Org. Chem.* 17 (2013) 2796–2813.
- [3] J. Handzlik, P. Sautet, *J. Catal.* 256 (2008) 1–14.
- [4] X.J. Li, D.Z. Zhang, X.X. Zhu, F.C. Chen, S.L. Liu, S.J. Xie, L.Y. Xu, *J. Mol. Catal. A: Chem.* 372 (2013) 121–127.
- [5] L. Harmse, C.V. Schalkwyk, E.V. Steen, *Catal. Lett.* 137 (2010) 123–131.
- [6] X.J. Li, W.P. Zhang, S.L. Liu, L.Y. Xu, X.W. Han, X.H. Bao, *J. Catal.* 250 (2007) 55–66.
- [7] S.J. Huang, F.C. Chen, S.L. Liu, Q.J. Zhu, X.X. Zhu, W.J. Xin, Z.C. Feng, C. Li, Q.X. Wang, L.Y. Xu, *J. Mol. Catal. A: Chem.* 267 (2007) 224–233.
- [8] J.C. Hu, Y.D. Wang, L.F. Chen, R. Richards, W.M. Yang, Z.C. Liu, W. Xu, *Micropor. Mesopor. Mater.* 93 (2006) 158–163.
- [9] J.L. Hérisson, Y. Chauvin, *Makromol. Chem.* 141 (1971) 161–176.
- [10] H. Aritani, O. Fukuda, T. Yamamoto, T. Tanaka, Y. Oakamoto, S. Imamura, *Chem. Lett.* 29 (2000) 66–67.
- [11] J. Handzlik, J. Ogonowski, J. Stoch, M. Mikolajczyk, *Catal. Lett.* 101 (2005) 65–69.
- [12] K. Zama, Y. Imada, A. Fukuoka, M. Ichikawa, *Appl. Catal. A: Gen.* 194 (2000) 285–296.
- [13] S.L. Liu, S.J. Huang, W.J. Xin, J. Bai, S.J. Xie, L.Y. Xu, *Catal. Today* 93 (2004) 471–476.
- [14] X.J. Li, W.P. Zhang, S.L. Liu, S.J. Xie, X.X. Zhu, X.H. Bao, L.Y. Xu, *J. Mol. Catal. A: Chem.* 313 (2009) 38–43.
- [15] X.J. Li, W.P. Zhang, X. Li, S.L. Liu, H.J. Huang, X.W. Han, L.Y. Xu, X.H. Bao, *J. Phys. Chem. C* 113 (2009) 8228–8233.
- [16] S.L. Liu, X.J. Li, W.J. Xin, S.J. Xie, P. Zeng, L.X. Zhang, L.Y. Xu, *J. Nat. Gas Chem.* 19 (2010) 482–486.
- [17] Y.D. Wang, Q.L. Chen, W.M. Yang, Z.K. Xie, W. Xu, D.Y. Huang, *Appl. Catal. A: Gen.* 250 (2003) 25–37.
- [18] H. Aritani, O. Fukuda, A. Miyaji, S. Hasegawa, *Appl. Surf. Sci.* 180 (2001) 261–269.
- [19] D.P. Debecker, P.H. Mutin, *Chem. Soc. Rev.* 41 (2012) 3624–3650.
- [20] D.P. Debecker, K. Bouchmella, C. Poleunis, P. Eloy, P. Bertrand, E.M. Gaigneaux, P.H. Mutin, *Chem. Mater.* 21 (2009) 2817–2824.
- [21] D.P. Debecker, B. Schimmoeller, M. Stoyanova, C. Poleunis, P. Bertrand, U. Rodemerck, E.M. Gaigneaux, *J. Catal.* 277 (2011) 154–163.
- [22] D.P. Debecker, M. Stoyanova, U. Rodemerck, P. Eloy, A. Léonard, B.L. Su, E.M. Gaigneaux, *J. Phys. Chem. C* 114 (2010) 18664–18673.
- [23] N. Liu, S. Ding, Y. Cui, N. Xue, L. Peng, X. Guo, W. Ding, *Chem. Eng. Res. Des.* 91 (2013) 573–580.
- [24] S.J. Huang, H.J. Liu, L. Zhang, S.L. Liu, W.J. Xin, X.J. Li, S.J. Xie, L.Y. Xu, *Appl. Catal. A: Gen.* 404 (2011) 113–119.
- [25] T.C. Sheng, S. Lang, B.A. Morrow, I.D. Gay, *J. Catal.* 148 (1994) 341–347.
- [26] B. Hu, I.D. Gay, *J. Phys. Chem. B* 105 (2001) 217–219.
- [27] M. Niwa, N. Katada, Y. Murakami, *J. Phys. Chem.* 94 (1990) 6441–6445.
- [28] K. Chen, S. Xie, A.T. Bell, E. Iglesias, *J. Catal.* 198 (2001) 232–242.
- [29] A. Christodoulakis, S. Boghosian, *J. Catal.* 260 (2008) 178–187.
- [30] R.L. Cordero, A.L. Agudo, *Appl. Catal. A: Gen.* 202 (2000) 23–35.
- [31] S. Rajagopal, H.J. Marini, J.A. Marzari, R. Miranda, *J. Catal.* 147 (1994) 417–428.
- [32] J. Handzlik, J. Ogonowski, J. Stoch, M. Mikolajczyk, *Appl. Catal. A: Gen.* 273 (2004) 99–104.
- [33] Z.F. Yan, J.Y. Fan, Z.J. Zuo, Z. Li, J.S. Zhang, *Appl. Surf. Sci.* 288 (2014) 690–694.
- [34] T. Hahn, U. Bentrup, M. Armbrüster, E.V. Kondratenko, D. Linke, *ChemCatChem* 6 (2014) 1664–1672.
- [35] H.J. Liu, S.J. Huang, L. Zhang, S.L. Liu, W. Wang, W.J. Xin, S.J. Xie, L.Y. Xu, *Chin. J. Catal.* 29 (2008) 513–518.
- [36] D.P. Debecker, M. Stoyanova, U. Rodemerck, A. Léonard, B.L. Su, E.M. Gaigneaux, *Catal. Today* 169 (2011) 60–68.
- [37] R. Thomas, J.A. Moulijn, V.H.J. De Beer, J. Medema, *J. Mol. Catal. A: Gen.* 255 (2003) 133–142.
- [38] A. Spamer, T.I. Dube, D.J. Moodley, C.V. Schalkwyk, J.M. Botha, *Appl. Catal. A: Gen.* 255 (2003) 133–142.
- [39] A.G. Gayubo, J.M. Arandes, A.T. Aguayo, M. Olazar, J. Bilbao, *Ind. Eng. Chem. Res.* 32 (1993) 588–593.
- [40] P.E. Eberly, C.N. Kimberli, W.H. Miller, H.V. Drushel, *Ind. Eng. Chem., Prod. Des. Dev.* 5 (1966) 193–198.
- [41] J. Bilbao, A.T. Aguayo, J.M. Arandes, *Ind. Eng. Chem., Prod. Des. Dev.* 24 (1985) 531–537.
- [42] D. Eisenbach, E. Gallei, *J. Catal.* 56 (1979) 377–389.